


## Relative permeability water/oil measurements with polymer and brine on reservoir cores

Dagfinn Sleveland, Kåre Olav Vatne, Daniel Strand, Elin Austerheim, Ali Mehrabi, Helga Bårdsen, Anne Stavland, IRIS


Final report IRIS – 2016/110

Project number: 7752483  
Project title: Relative permeability water/oil measurements with polymer and brine on reservoir cores  
Client(s): The National IOR Centre of Norway  
Distribution restriction: Confidential

Stavanger, 2016.14.06

  
Dagfinn Sleveland 14/6-16  
Project Manager Sign.date

  
Arne Stavland 14/6-16  
Project Quality Assurance Sign.date

  
Hilde Carlsen Jonsbråten 14/6-16  
Manager, Petroleum laboratory Sign.date  
IRIS Energi



## Table of Contents

1	EXECUTIVE SUMMARY .....	7
2	INTRODUCTION.....	7
3	PLUG PREPARATION AND ANALYTICAL PROCEDURES.....	9
3.1	Core material .....	9
3.1.1	Initial plug preparations .....	9
3.1.2	Routine core measurements .....	9
4	TEST FLUIDS .....	10
4.1	Synthetic formation water.....	10
4.2	Isopar-H .....	10
4.3	Polymer.....	10
5	BASIC MEASUREMENTS .....	11
6	WHITE OIL/SFW DRAINAGE, AGEING WITH STO AND WETTABILITY TESTING .....	13
6.1	Introduction and key results.....	13
6.2	Oil/SWF-drainage.....	14
6.3	Ageing .....	15
6.4	Wettability testing .....	16
7	WATER-POLYMER/OIL – RELATIVE PERMEABILITY – STEADY STATE .....	18
7.1	Introduction .....	18
7.2	Polymer.....	18
7.2.1	Polymer used.....	18
7.2.2	Shear test.....	18
7.2.3	Pre-shearing of final polymer solution.....	21
7.2.4	Filter tests.....	21
7.3	Experimental procedure .....	22
7.3.1	Mounting and preparing composite core .....	22
7.3.2	Relative permeability by steady-state flooding using SFW and polymer .....	22
7.3.3	Final measurements .....	22
7.4	Composite core.....	22
7.5	Initial core measurements and parameters .....	23
7.6	Key results.....	24
7.7	Comments.....	27
7.8	Interpretations.....	28

8	APPENDIX.....	30
APPENDIX A	LIST OF SYMBOLS.....	30
APPENDIX B	ACRONYMS AND SPECIAL TERMS.....	33
APPENDIX C	STEADY-STATE RELATIVE PERMEABILITY MEASUREMENT.....	34
C.1	Introduction: Steady-state relative permeability .....	34
C.2	Apparatus Overview .....	34
C.3	Pumping System .....	35
C.4	Fluid Separator .....	35
C.5	Hydrostatic core holder .....	36
C.6	Pressure difference.....	37
C.7	Water/Oil Kr SS – Flooding apparatus. ....	37

## List of figures

Figure 1-1: Test program, flow chart .....	8
Figure 4-1: $k_w$ versus $\Phi_{Mohr}$ .....	12
Figure 5-1: Schematic view of experimental setup.....	14
Figure 5-2: Ageing – increase in RI over time.....	15
Figure 5-3: $k_o(S_{wi})$ before ageing versus $k_o(S_{wi})$ after ageing .....	16
Figure 5-4: Wettability test – spontaneous imbibition of samples vs very strongly water wet outcrop core.....	17
Figure 6-1: Degradation test of polymer. Recirculation through pump and background. ....	19
Figure 6-2: Degradation test of polymer. Shearing of batch sample with Silverson LSM.....	20
Figure 6-3: Degradation test in pump using pre-sheared polymer. ....	20
Figure 6-4: Pre-shearing of final polymer solution.....	21
Figure 6-5: $k_{rw}$ and $k_{ro}$ for composite core C .....	24
Figure 6-6: SFW/polymer saturation during SS-flooding.....	25
Figure 6-7: Transient data of oil production and dP during SS-experiment .....	25
Figure 7-8: Measured and estimated fractional flow.....	28
Figure 6-9: Polymer bulk viscosity fitted with a power law dependency .....	29
Figure 7-1: Apparatus for Two-phase Steady State Core Flooding. ....	35
Figure 7-2: Separator used in recirculating core flood system.....	36
Figure 7-3: Hydrostatic Core Holder – Principle. ....	36
Figure 7-4: Water/Oil Kr SS flooding rig.....	37

**List of tables**

---

<i>Table 3-1: Brine composition and specifications.....</i>	<i>10</i>
<i>Table 4-1: Basic measurements for all plugs.....</i>	<i>11</i>
<i>Table 5-1: Capillary drainage tests, gas/water &amp; end-point saturation exponents (n), key results. 13</i>	
<i>Table 5-2: Wettability test – spontaneous imbibition.....</i>	<i>17</i>
<i>Table 6-1: Composite core C.....</i>	<i>22</i>
<i>Table 6-2: Composite core C for Water-Polymer/Oil Kr SS tests.....</i>	<i>23</i>
<i>Table 6-3: Water-polymer/Oil Kr SS for composite core C.....</i>	<i>24</i>
<i>Table 6-4: Flooding with SFW after SS-experiment.....</i>	<i>26</i>
<i>Table 6-5: Saturation measurements.....</i>	<i>26</i>

## 1 Executive summary

This work, part of the National IOR centre of Norway, aimed to demonstrate how data from special core analysis can be utilized to demonstrate EOR potential.

Reservoir cores, previously used for SCAL were reprepared, drained to  $S_{wi}$  and aged with STO.

Steady state water/oil relative permeability was performed at increasing fractional flow. At water fractional flow of  $f_w=0.22$ , brine was replaced with viscous polymer which revealed a significant shift in water saturation. The water and polymer fractional flow curves were well matched with standard fractional flow curves.

## 2 Introduction

The work has been done in accordance with updated routines existing for special core analyses at IRIS Core laboratory. The technical equipment and precision instruments used for the analyses are calibrated and tested on a routine basis. IRIS complies with Environmental Management System Standard NS-EN ISO 14001:2004 and with Quality Systems Standard NS-EN ISO 9001. Further information can be obtained from our Quality Assurance manual.

*Figure 2-1* shows a flow chart for the work program.

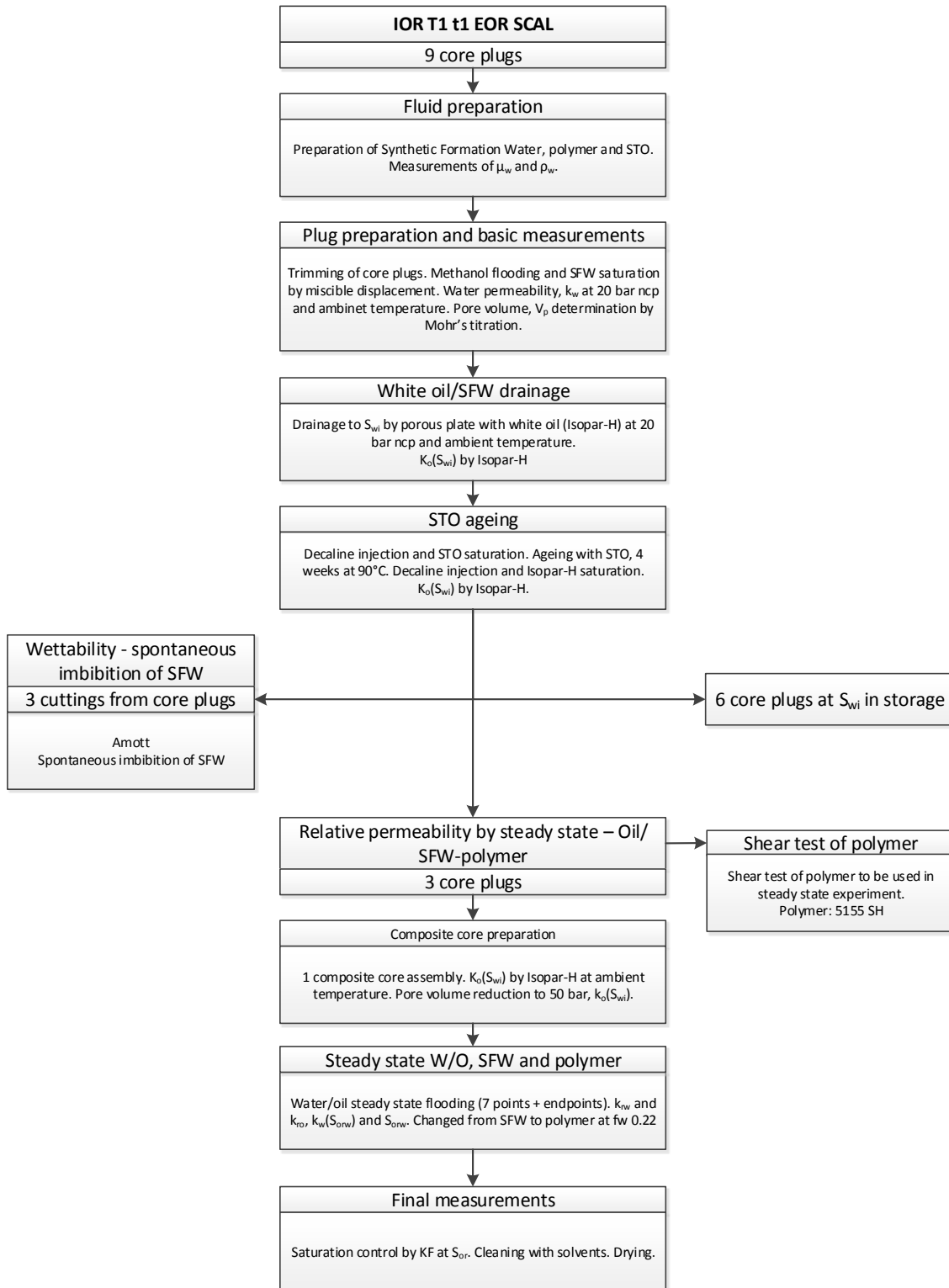


Figure 2-1: Test program, flow chart



## **3 Plug preparation and analytical procedures**

### **3.1 Core material**

9 1.5'' cores from a well drilled from a NSC field was released by Statoil for use in this project. The cores had previously been through a SCAL-program at IRIS and were stored at IRIS. The cores were stored in a dry state.

#### **3.1.1 Initial plug preparations**

The plugs had been trimmed before the SCAL-program, but the plugs were retrimmed at the start of this program because of some grain loss at the plug ends. The cores were mounted in core holders with a confining pressure of 20 bar. The plugs were flooded with methanol to remove air before they were saturated with SFW by miscible displacement.

#### **3.1.2 Routine core measurements**

After saturation the absolute permeability ( $k_w$ ) of the plugs to SFW were measured at room temperature and 20 bar net confining pressure (NCP). Afterward pore volume (PV) and porosity were determined by nitrate flooding and Mohr's titration at room temperature and 20 bar NCP. The plugs were then flooded with SFW to displace the nitrate formation water at ambient conditions at 20 bar NCP.

## 4 Test fluids

### 4.1 Synthetic formation water

The synthetic formation water was made from chlorides of Na, Ca, Mg, K and Sr as per the composition listed below. The brine was filtered through 0,45  $\mu\text{m}$  filter and degassed before use. The physical properties of the brine used in this program are given in *Table 4-1*. The viscosity and density of the brine were measured at ambient temperature.

*Table 4-1: Brine composition and specifications*

Recipe given by Statoil:	Salt	Amount [g/L]
	CaCl <sub>2</sub> · 2H <sub>2</sub> O:	35,768
	KCl:	3,501
	MgCl <sub>2</sub> · 6H <sub>2</sub> O:	8,538
	SrCl <sub>2</sub> · 6H <sub>2</sub> O:	3,347
	NaCl:	104,999
Brine specifications:	Density (at 23 °C):	1,0983 [g/mL]
	Viscosity (at 20 °C):	1,348 [cP]

### 4.2 Isopar-H

The white oil, Isopar-H, were used in drainage to  $S_{wi}$  and permeability measurements. The viscosity of Isopar-H at 20 °C and ambient pressure were measured to be: 1,218 cP.

### 4.3 Polymer

A synthetic polymer from SNF, 5115 SH, were used in this project. A mother solution of 5000 ppm was made and diluted with brine to a concentration of 1000 ppm and 1750 ppm. See section 7.2 for further details.

## 5 Basic measurements

The basic measurements prior to the tests are presented in *Table 5-1*. The initial basic measurements include absolute permeability to water at 20 bar ncp, bulk volume, pore volume, and porosity. Because GV,  $BV_{Hg}$  or 0-20 bar pore squeeze have not been measured, BV is based on length and diameter measurements using calipers at atmospheric conditions. This gives a slightly too low porosity. These data were not used in the calculations for the steady state experiment.

Nitrate flooding followed by Mohr's titration was used to determine the pore volume and porosity of the plugs.

*Table 5-1: Basic measurements for all plugs*

IRIS Plug ID	Core <sup>1)</sup>	L	D	BV <sup>2)</sup>	PV <sub>Mohr</sub>	$\phi$ <sub>Mohr</sub>	Kw
				atm	20 bar	20 bar	20 bar
		[cm]	[cm]	[mL]	[mL]	[frac.]	[mD]
220	A1	7,63	3,803	86,68	20,06	0,231	884
221	A2	6,10	3,809	69,51	15,65	0,225	914
222	A3	6,91	3,809	78,74	19,73	0,251	799
230	B1	6,67	3,809	75,97	17,03	0,224	1330
233	B2	7,65	3,812	87,29	19,93	0,228	1486
235	B3	6,42	3,810	73,21	16,48	0,225	1136
226	C1	7,82	3,812	89,21	20,88	0,234	1507
237	C2	7,28	3,807	82,90	19,65	0,237	1724
199	C3	7,72	3,807	87,91	21,32	0,242	1531

<sup>1)</sup> Depths removed. Each letter represents a seal peal.

<sup>2)</sup> BV based on caliper at atmospheric conditions. Porosities will be slightly too low.

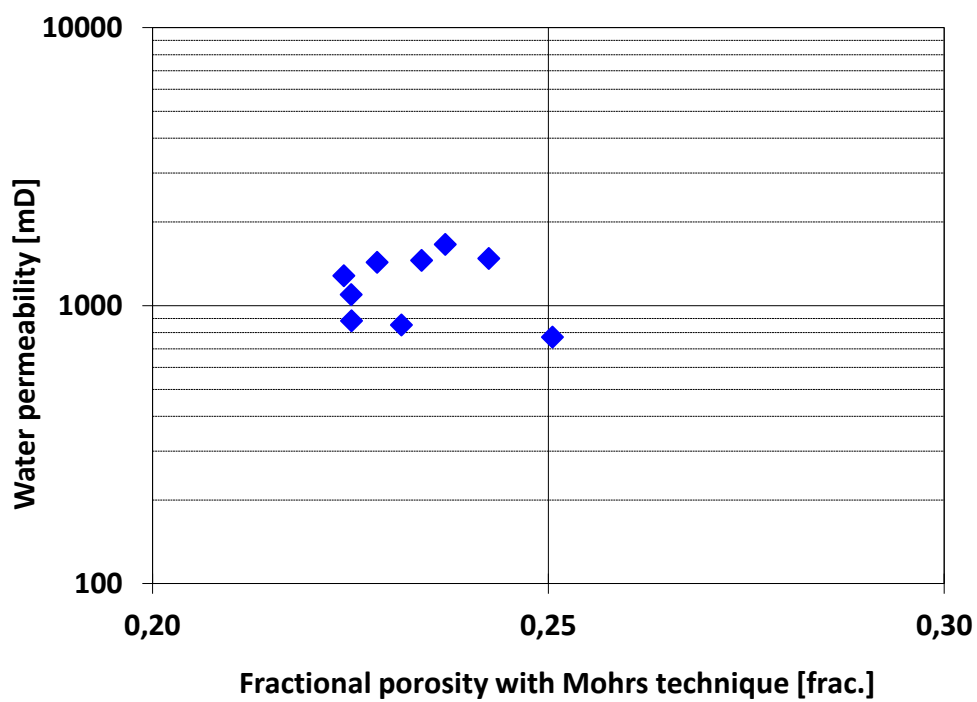


Figure 5-1:  $k_w$  versus  $\Phi_{Mohr}$

## 6 White oil/SFW drainage, ageing with STO and wettability testing

### 6.1 Introduction and key results

$S_{wi}$  was established by individual porous plate drainage at 5 bar capillary pressure with white oil at 20 bar NCP and ambient temperature. Isopar-H was used as the white oil.

After removal of the porous plates, the oil permeability at  $S_{wi}$  was determined.

Decaline was then injected as a buffer before injecting stock tank oil so as not to precipitate heavy oil components. The cores were aged at 90 °C for four weeks while the resistivity through the core was monitored. The stock tank oil was changed once half way through the ageing process. When the resistivity was stable after changing the STO, the STO was removed by injecting decaline and then isopar-H.

$K_o(S_{wi})$  was remeasured using isopar-H after the ageing was finished.

Table 6-1 shows the measured end-point saturations based on the mass balance from oil-water drainage and the oil permeabilities before and after ageing.

Table 6-1: Capillary drainage tests, gas/water & end-point saturation exponents ( $n$ ), key results

IRIS Plug ID	Core <sup>1)</sup>	L	D	BV <sup>2)</sup>	PV <sub>Mohr</sub>	$\phi$ <sub>Mohr</sub>	Kw	S <sub>wi</sub>	$k_o(S_{wi})$ <sub>Isopar</sub> Before ageing	$k_o(S_{wi})$ <sub>Isopar</sub> After ageing
		[cm]	[cm]	atm	20 bar	20 bar	20 bar	20 bar	20 bar	20 bar
		[mL]	[mL]	[frac.]	[mD]	[frac.]	[mD]	[mD]	[mD]	
220	A1	7,63	3,803	86,68	20,06	0,231	853	0,113	798	790
221	A2	6,10	3,809	69,51	15,65	0,225	882	0,133	617	775 <sup>3)</sup>
222	A3	6,91	3,809	78,74	19,73	0,251	772	0,129	665	653
230	B1	6,67	3,809	75,97	17,03	0,224	1284	0,109	1244	1218
233	B2	7,65	3,812	87,29	19,93	0,228	1434	0,113	1441	1436
235	B3	6,42	3,810	73,21	16,48	0,225	1096	0,125	1175	1151
226	C1	7,82	3,812	89,21	20,88	0,234	1454	0,070	1516	1560
237	C2	7,28	3,807	82,90	19,65	0,237	1663	0,064	1669	1680
199	C3	7,72	3,807	87,91	21,32	0,242	1478	0,069	1690	1682

<sup>1)</sup> Depths removed. Each letter represents a seal peal.

<sup>2)</sup> BV based on caliper at atmospheric conditions. Porosities will be slightly too low.

<sup>3)</sup> Measured twice

After the ageing was finished and the cores were saturated with isopar-H again, a part of one core from each seal peal was removed and put into an Amott-beaker for spontaneous imbibition of SFW to test the achieved wettability.

## 6.2 Oil/SWF-drainage

Semi permeable ceramic porous plates were installed at the downstream end of each core plug. To maintain hydraulic contact between plug's surface and porous plate, kaolinite paste was applied. At a constant confining pressure of 20 bar and ambient temperature, the plugs were drained to irreducible water saturations ( $S_{wi}$ ) with isopar-H allowing for a maximum water production of 1 mL/day for each individual plug. The capillary pressure was increased in 8 steps from 0 to 5 bar.

Electrical resistivity measurements were performed during the drainage. The samples were exposed to a known current frequency of 1 kHz with a two-point electrode system. The impedance and the phase angle were recorded for each sample, allowing calculation of the electrical sample resistivity.

The experimental setup used during the drainage is shown in *Figure 6-1*.

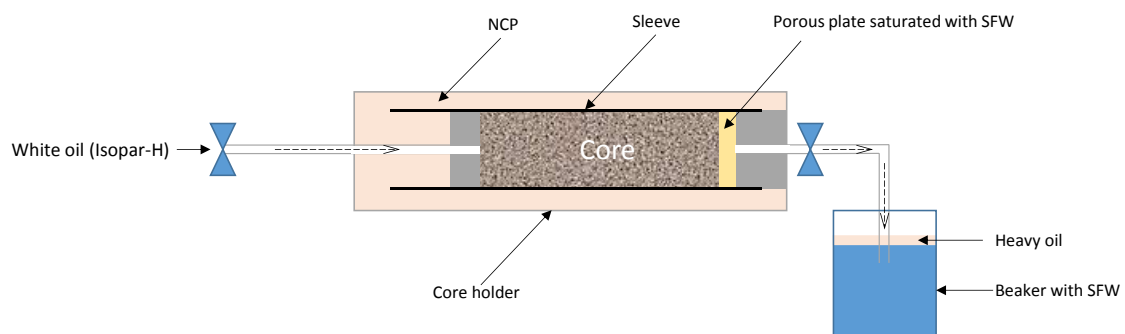


*Figure 6-1: Schematic view of experimental setup*

At the end of the drainage, the porous plates were removed and relative permeability to isopar-H ( $k_o(S_{wi})$ ) was measured at ambient conditions.

### 6.3 Ageing

The cores were then flooded with decaline to displace all isopar-H and the core holders mounted in a heating cabinet. The temperature was increased to 60 °C and 2 pore volumes of STO was injected in each core. The STO used was an old separator sample from a Norwegian oil field, but not the same as which the core material originated from. The decaline acted as a buffer to keep any heavy oil components in the STO from precipitating in contact with the isopar-H. When all cores had been flooded with STO the temperature was increased to 90 °C for 4 weeks. Another 2 pore volumes of STO was injected after 13 days.

Figure 6-2 show how the RI changes over time during the ageing process. The six cores from seal peal A and B hardly experience any ageing effect, while all three cores from seal peal C experience an increase in RI which indicate an increased oil-wetness. The three cores from seal peal C also show a marked increase in RI after the STO was changed after 13 days.

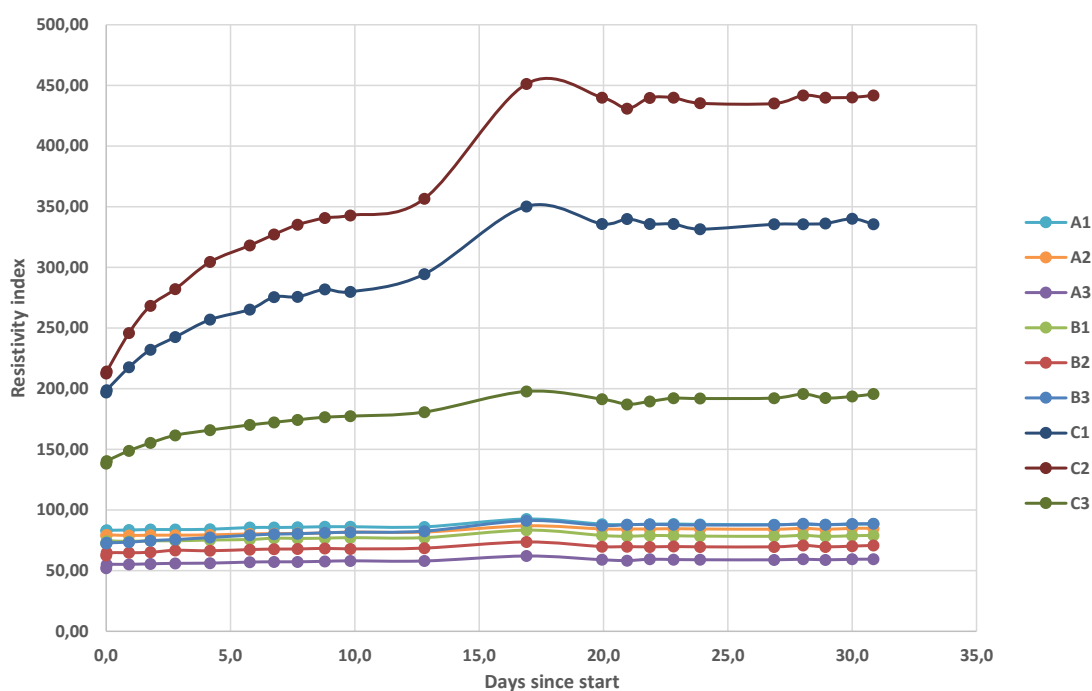


Figure 6-2: Ageing – increase in RI over time

Figure 6-3 show the relationship between the ( $k_o(S_{wi})$ ) before and after ageing. There was a good match between the two measurements, except for core A2, which had significantly higher permeability after ageing. Based on the rest of the data it would seem the measurement of ( $k_o(S_{wi})$ ) for A2 before ageing is too low.

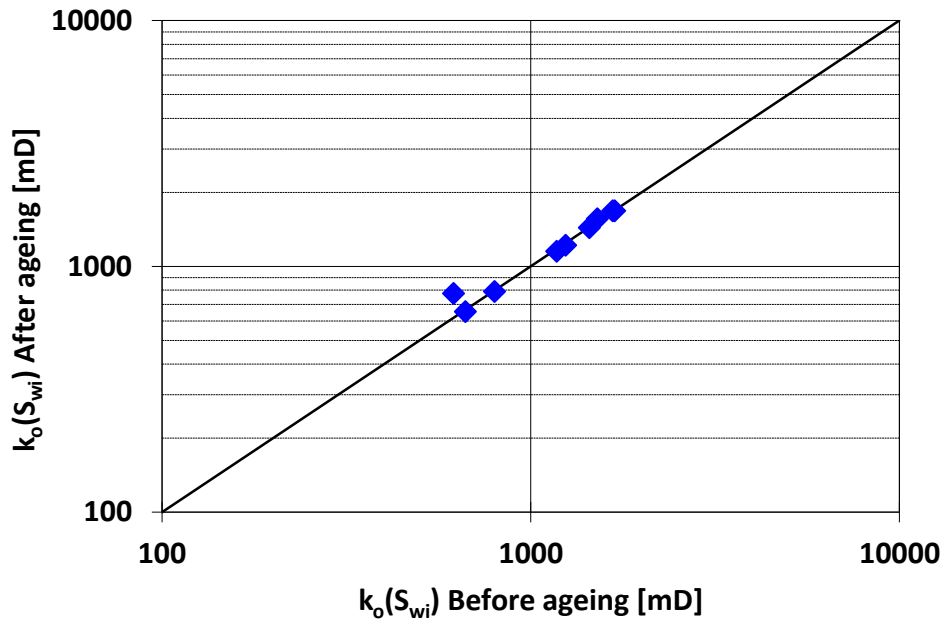


Figure 6-3:  $k_o(S_{wi})$  before ageing versus  $k_o(S_{wi})$  after ageing

## 6.4 Wettability testing

To have an indication of the achieved wettability it was decided to cut off part of three cores, one from each seal peal, and do spontaneous imbibition of SFW on them. The three selected cores were dismantled, a 2 cm section cut of one end and then the main core was wetmounted with isopar-H back in the core holder.

Only a small amount of material could be removed from the main cores since the composite core in the SS-experiment should have as long a core as possible. It was assumed that the porosity and saturation was constant through each core.

The cut-offs were put into Amott-beakers filled with SFW and the production of oil (imbibition of SFW into the cores) was monitored by reading produced oil volume in a graduated cylinder.

Table 6-2 show the production of oil from the three cores. There were problems with oil drops sticking to the cores and glas walls giving too low recorded oil production, especially for A1 which had no oil production recorded. Based on visual observation of the droplets stuck to the cores and glas, the the missing production would still be low (< 0,4 mL).



Table 6-2: Wettability test – spontaneous imbibition

t [min]	A1			B2			C1		
	t <sub>D</sub>	ΔV <sub>o</sub> [mL]	Recovery [frac.]	t <sub>D</sub>	ΔV <sub>o</sub> [mL]	Recovery [frac.]	t <sub>D</sub>	ΔV <sub>o</sub> [mL]	Recovery [frac.]
0	0	0,00	0,00	0	0,00	0,00	0	0,00	0,00
60	3850	0,00	0,00	5183	0,10	0,02	4959	0,00	0,00
120	7701	0,00	0,00	10366	0,10	0,02	9918	0,00	0,00
1080	69304	0,00	0,00	93292	0,15	0,03	89265	0,05	0,01
2760	177111	0,00	0,00	238412	0,15	0,03	228122	0,07	0,01
4500	288769	0,00	0,00	388716	0,15	0,03	371937	0,10	0,02
18495	1186839	0,00	0,00	1597623	0,15	0,03	1528662	0,10	0,02

t<sub>D</sub> - Dimensionless time

Production somewhat too low, especially for A1, because of oil sticking to the cores and glass walls.

Figure 6-4 show the oil recovery for the three cores plotted against dimensionless time. The production curve of a very strongly water wet outcrop core is also plotted (black line). Comparing the production from the core samples with the production curve of the very strongly water wet outcrop core, it indicates that the ageing with STO have made the cores oil wet.

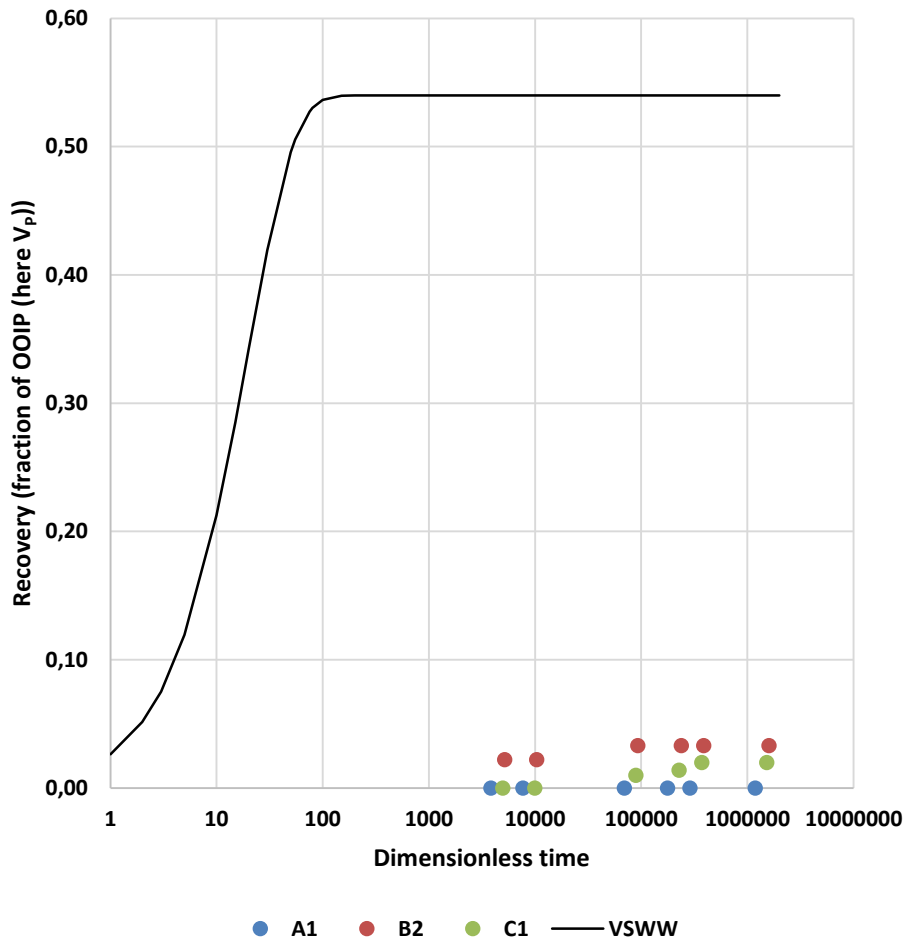


Figure 6-4: Wettability test – spontaneous imbibition of samples vs very strongly water wet outcrop core

## 7 Water-polymer/Oil – Relative permeability – Steady State

### 7.1 Introduction

The cores from seal peal C was selected to be used in the SS-experiment, because they had the highest permeability and, based on RI from ageing with STO, were the most oil wet. The cores were stacked into a composite core and mounted in a single core holder.

The SS-experiment was started as a normal water/oil experiment, with the use of SFW initially for the first four fractions. When the production of oil was stable at the fourth fraction, the SFW-feed was changed to the polymer while keeping the fraction the same. When the oil production had stabilized again, the last five fractions were conducted using polymer. The polymer had been sheared down before use.

Finally the core was flooded with solvents to remove all water so the end water saturation could be determined by Karl Fischer titration.

### 7.2 Polymer

#### 7.2.1 Polymer used

A synthetic polymer from SNF, from called 5115 SH, was used in the SS-experiment. The end polymer was made from a 5000 ppm motherliquor of 5155 in SFW which was diluted to 1750 ppm using SFW.

The initial shear tests were conducted using a 1000 ppm polymer.

Polymers have variable viscosity based on the share rate they are exposed to. The viscosities given in section 7.2 are measured on an Anton Paar Physica MCR 301 rheometer at shear rate of 1 to 5 s<sup>-1</sup>. The effective viscosities during the SS-experiment have been addressed in section 7.8.

#### 7.2.2 Shear test

When a polymer pass constrictions its molecular structure can be sheared into smaller sections, reducing the viscosity of the fluid. How much the polymer is sheared is dependent on the size of the molecular chains, the size of the constriction, the speed the polymer flows past the constriction etc.

During the planning of the experiment is was discussed if the polymer would be recirculated through the rig or not. Since the polymer would meet many constrictions and sharp bends in the tubing and valves of the rig, the viscosity of freshly made polymer would be reduced drastically if it was recirculated through the pump system like the brine usually is. A few simple experiments were conducted to test how much the polymer would degrade because of shear and other factors.

A sample of 1000 ppm polymer was placed in a flask with a stirring magnet set at a minimal speed. The inlet line to a QX-6000 pump with BV valves was put inside the flask. The outlet from the pump went via an Autoklav valve and two CV-310 valves before going back into the flask. The rate was set to 1 mL/min with a returnrate of 1.2. Polymer samples were taken directly from the outlet tube throughout the test and the change in viscosity was determined.

Since other factors than the recirculation through the pump also can lead to degradation of the polymer a parallel test was started with a similar flask, polymer amount, magnetic stirrer size and speed some hours after the first test had been started.

Figure 7-1 show a substantial reduction in viscosity in the sample being recirculated through the pump, but that some of the reduction is caused by other effects, like the magnetic stirring bar and temperature.

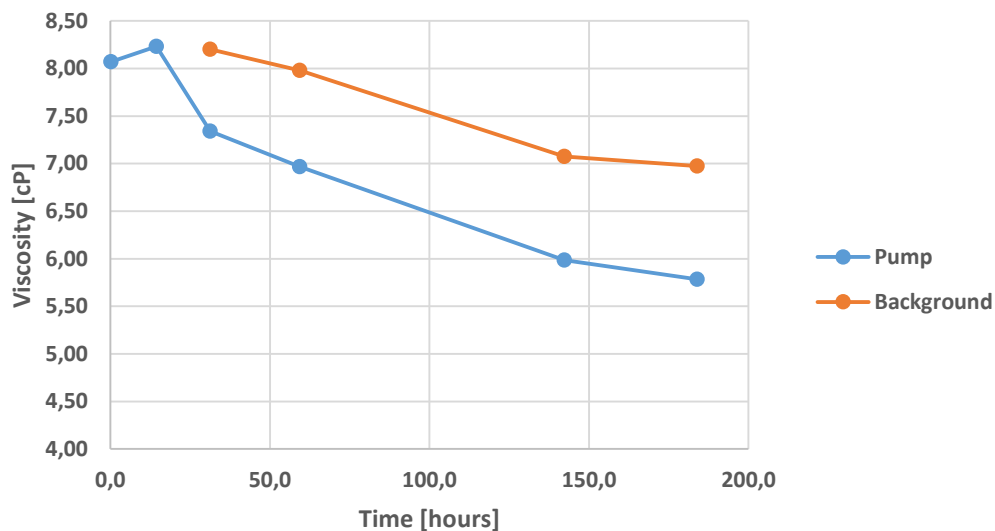


Figure 7-1: Degradation test of polymer. Recirculation through pump and background.

By pre-shearing the polymer before using it in the SS-rig problems with degradation of the polymer can be minimized. A degradation test was run on a batch sample using a Silverson L5M equipped with a ring with 2,6x2,4 mm square holes, using 3 different speeds. The goal was to reach a lower viscosity than the recirculation test had produced. Figure 7-2 show the degradation of a larger 1000 ppm polymer sample using three different speeds.

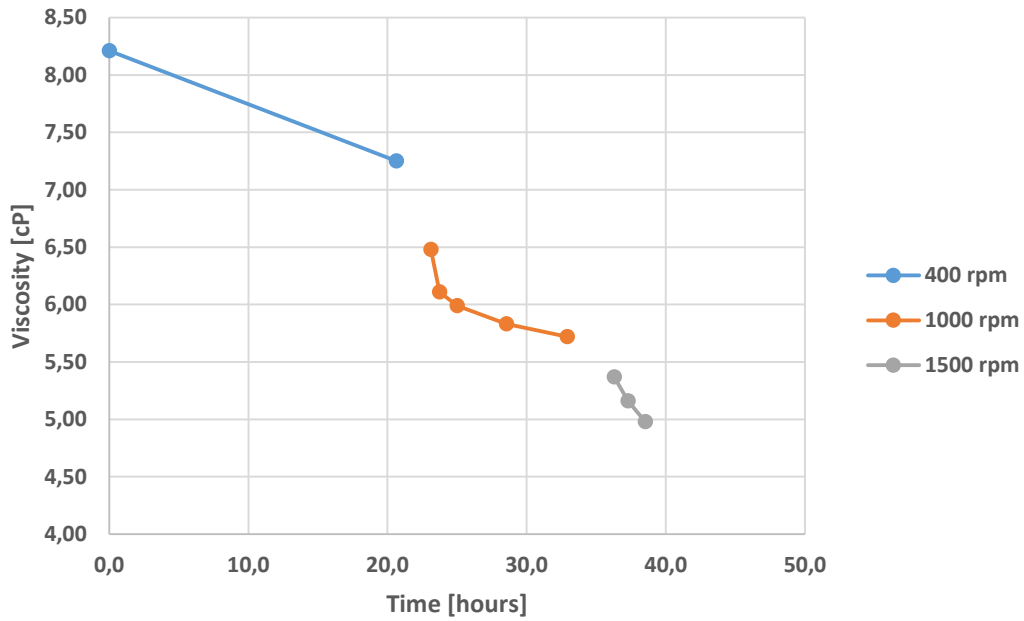


Figure 7-2: Degradation test of polymer. Shearing of batch sample with Silverson L5M.

To check if the pre-sheared polymer from the above test would be more or less stable in the SS-rig, a pre-sheared sample (from the test above) was tested with recirculation through the same pumpsetup as initially described. The test shows that the viscosity of the sample is stable for a long time in the pump after it has been pre-sheared.

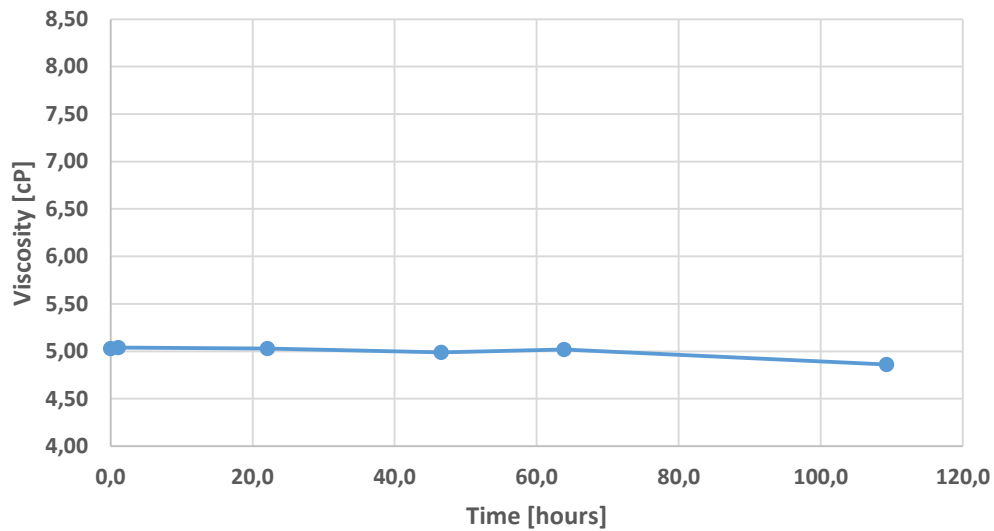
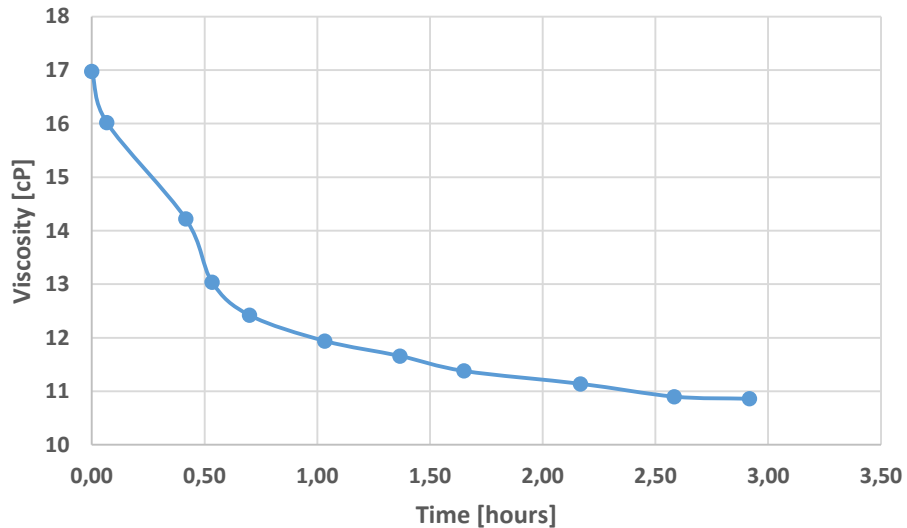


Figure 7-3: Degradation test in pump using pre-sheared polymer.

### 7.2.3 Pre-shearing of final polymer solution

The end viscosity of a 1000 ppm polymer after pre-shearing was deemed a little low, so the concentration was increased to 1750 ppm. This sample was pre-sheared using the Silverson L5M at 1500 rpm and was used in the final SS-experiment. *Figure 7-4* shows the change in viscosity during the pre-shearing over time.



*Figure 7-4: Pre-shearing of final polymer solution.*

### 7.2.4 Filter tests

The SS-rig have in-line filters of 3,0  $\mu\text{m}$  which the polymer must pass through if it is being recirculated. A 1000 ppm 5115 SH polymer solution was tested against filters with different pore sized, but there was little or no effect on the viscosity.

## 7.3 Experimental procedure

An overview of the program for relative permeability measurements is given in *Figure 2-1* (page 8). The apparatus for steady-state flooding tests is presented in Appendix C.

### 7.3.1 Mounting and preparing composite core

- Assembling the plugs into composite core
- Measurement of  $k_o(S_{wi})$  flooding with isopar-H at 21°C.
- Pore volume reduction to 50 bar,  $k_o(S_{wi})$ .

### 7.3.2 Relative permeability by steady-state flooding using SFW and polymer

- Horizontal injection
- Monotonously increase water flow-fraction up to 0,2
- When stable production, change from brine to polymer, still at flow-fraction 0,2
- Continue monotonously increase of polymer flow-fraction up to 1,0
- Bumpflooding with SFW

### 7.3.3 Final measurements

- Water content measurement by Karl Fischer
- Cleaning by flooding alternating solvent (60 °C)
- Drying

## 7.4 Composite core

The cores from seal peal C was selected to be used in the SS-experiment, because they had the highest permeability and, based on RI from ageing with STO, were the most oil wet. The cores were stacked into a composite core and mounted in a single core holder, see *Table 7-1*. The cores are stacked from highest to lowest permeability, with the highest permeability towards the inlet.

*Table 7-1: Composite core C*

IRIS Plug ID	Core*	L	D	Kw	ko(Swi) Isopar	ko(Swi) Isopar	Composite Order
		[cm]	[cm]	20 bar	Before ageing	After ageing	
		[cm]	[cm]	[mD]	20 bar	20 bar	
		[mD]	[mD]	[mD]			
226	C1	5,70 <sup>1)</sup>	3,812	1454	1516	1560	3
237	C2	7,28	3,807	1663	1669	1680	2
199	C3	7,72	3,807	1478	1690	1682	1

<sup>1)</sup>Core C1 have been cut to new length because of sample for spont. imb.

## 7.5 Initial core measurements and parameters

Composite core C is described in *Table 7-2*.

*Table 7-2: Composite core C for Water-Polymer/Oil Kr SS tests*

Name		Composite core C
Length	[cm]	20,71
Diameter	[cm]	3,81
Pore volume	[mL]	55,81
$S_{wi}$	[frac.]	0,068
$S_{or}$	[frac.]	0,167
$k_{o(20 \text{ bar NCP})(S_{wi})}$	[mD]	1616
$k_{o(50 \text{ bar NCP})(S_{wi})}$	[mD]	1591
$k_{REF}$	[mD]	1591

$\phi$	Pore volume and porosity based on Mohrs titration.
$S_{wi}$	Initial water saturation as established for the composite core established on porous plate.
$S_{or}$	Residual oil saturation.
$K_{o(20 \text{ bar NCP})(S_{wi})}$	Permeability to oil at 20 bar NCP and $S_{wi}$ at ambient temperature.
$K_{o(50 \text{ bar NCP})(S_{wi})}$	Permeability to oil at 50 bar NCP and $S_{wi}$ at ambient temperature.
$k_{REF}$	Reference permeability used in relative permeability calculations.

## 7.6 Key results

Table 7-3 show the detailed results for each flow fraction. Figure 7-5 show the relative permeabilities for water/polymer and oil.

Table 7-3: Water-polymer/Oil Kr SS for composite core C

Field:	-	Test:	Steady state flooding	$L_c$	20,71 cm	$P_p$	20 bar	
Well:	-	Conditions:	Ambient	PV	55,81 mL	$\mu_w$	1,248 cP	
Plug:	C	Process:	W/O – Horizontal	$K_{ref}$	1591 mD	$\mu_o$	1,229 cP	
							$\mu_{poly}$	7,0 cP
Water-polymer/Oil Kr SS (Increasing water/polymer - Decreasing oil)								
$V_{pinj}$	$q_t$	$f_w$	$S_w$	$k_{rw}$	$k_{rg}$			
[PV]	[mL/h]	[frac.]	[frac.]	[frac.]	[frac.]			
0,0	360	0,000	0,068	0,0000	1,0000			
100,6	120	0,008	0,168	0,0046	0,5625			
52,6	120	0,060	0,205	0,0206	0,3182			
65,4	120	0,220	0,329	0,0628	0,2195			
88,9	120	0,220	0,535	0,1321	0,0822			
40,8	90	0,500	0,600	0,1800	0,0316			
27,6	60	0,780	0,660	0,1808	0,0090			
28,3	60	0,940	0,719	0,1924	0,0022			
20,7	60	0,984	0,753	0,1723	0,0005			
26,9	60	1,000	0,833	0,1532	0,0000			

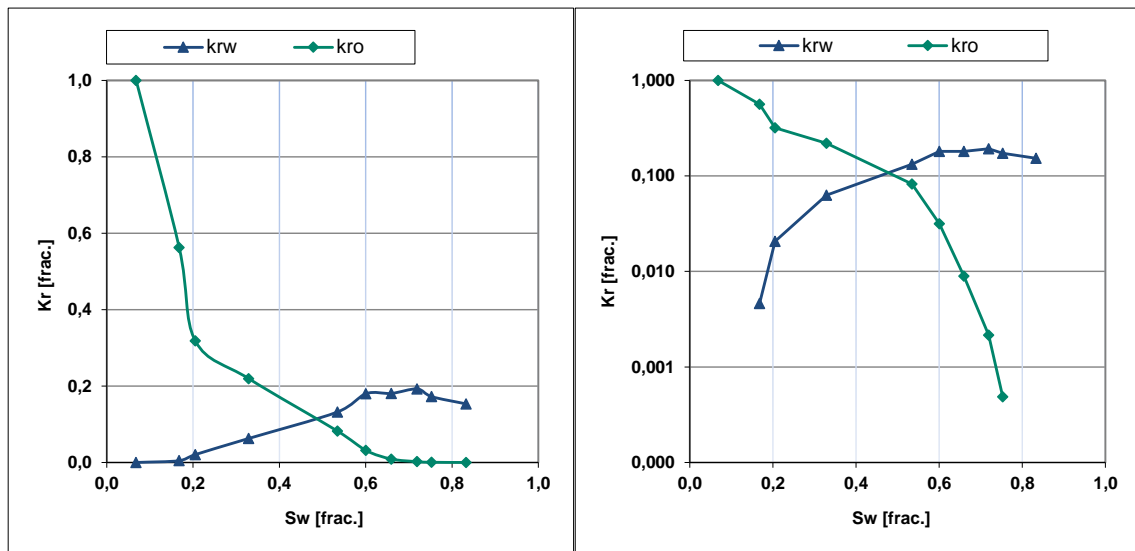


Figure 7-5:  $k_{rw}$  and  $k_{ro}$  for composite core C



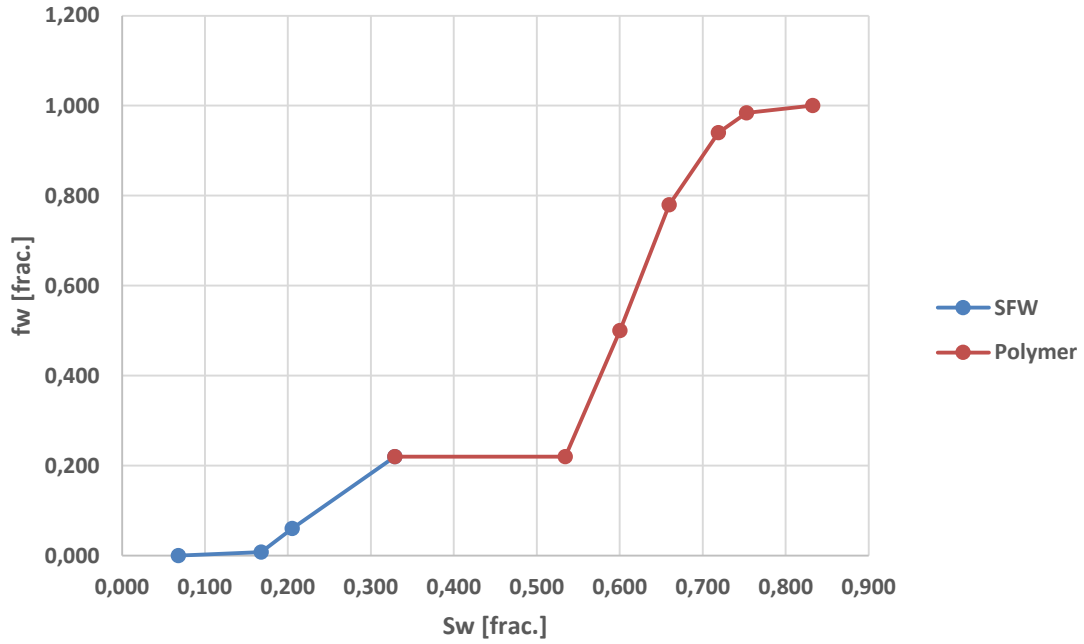


Figure 7-6: SFW/polymer saturation during SS-flooding

Figure 7-6 show the SFW/polymer end saturations for each rate step. Figure 7-7 show the transient oil production and delta pressure data. Oil production is given as points at stable conditions for each rate step when flooding with polymer.

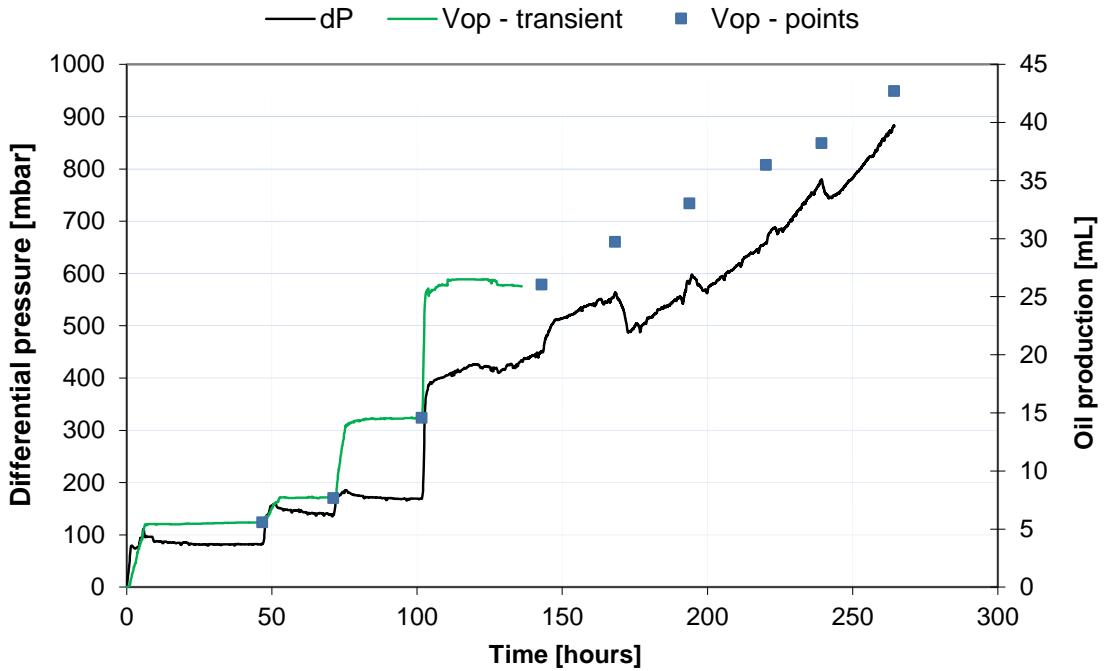


Figure 7-7: Transient data of oil production and dP during SS-experiment

After the SS-experiment were finished, the core was flooded with SFW to see if the plugging could be removed. Some extra oil was initially produced when first flooding with SFW. No more oil was produced at the higher rates. *Table 7-4* show rates, delta pressure and extra oil production.

*Table 7-4: Flooding with SFW after SS-experiment*

$q_{SFW}$ [mL/min]	$q_{Poly}$ [mL/min]	dP [mbar]	Extra oil production [mL]
0	1	882	0
1	0	1954	1,3
2	0	2220	1,3
4	0	2580	1,3
8	0	3155	1,3
15	0	3720	1,3

*Table 7-5* show two independent saturation measurements, one based on porous plate and volumetric balance and one from Karl Fischer at the end of the experiment. KF-data corrected for additional oil production during the bump flooding with SFW after the main SS-experiment have also been reported.

*Table 7-5: Saturation measurements*

Saturation measurements	$S_{wi}$ [frac.]	$S_{or}$ [frac.]
PP drainage & volumetric balance <sup>1)</sup>	0,068	0,167
Karl Fischer	0,090	0,145
Karl Fishcer - corrected for extra production	0,067	0,168

<sup>1)</sup> Used in calculations

## 7.7 Comments

The SFW used in the initial rate steps was recirculated through the SS-rig. The polymer was not recirculated through the rig, but was flooded through the core and separator and into a waste container. The oil was always recirculated.

In *Figure 7-7* continuous transient data for the volume of oil produced is not reported when flooding with polymer. This is because there was development of emulsion in the separator, making it very work intensive to do interpretation of the pictures of the separator. Instead of interpreting all the pictures, only the last pictures giving the volume at steady state before going to the next rate step was interpreted. In these interpretations the emulsion was ignored with regards to produced oil. These values are given as points in the figure.

As shown in *Figure 7-7* the dP would not stabilize at each rate step when flooding with polymer. The dP used in the calculations was the last value recorded before going to the next rate step.

After the last rate step using polymer was finished (first entry in *Table 7-4*), SFW was injected with increasingly higher rates to see if the blockage of the cores could be removed, but there was no marked reduction in dP to indicate this. There was some extra oil production when first changing to SFW, but there was no more oil production at the higher rates.

Since the Karl Fischer flooding is done after the rate bump with SFW, the extra oil production must be compensated for to get the true saturation at the end of the experiment. In *Table 7-5* both values are listed. The values from porous plate with volumetric balance correspond very well with the corrected Karl Fischer data, confirming that the volumes read from the separator were correct. The Kr-calculations have been based on the porous plate and volumetric balance data.

Because the blockage could not be removed, the total pore volume of the composite core was not measured on the dried composite plug as customary.

## 7.8 Interpretations

The following interpretations was made:

1. Adjust the water/oil relative permeability curves to match Corey-type relative permeability curves. From the oil-water SS experiments at fractional flow up to  $f_w = 0.22$  a proper match was found by setting the water and oil Corey exponents equal to 1.75 and 3.6, respectively. The endpoint oil and water permeabilities was set equal to 1.0 and 0.5, respectively.
2. During the oil-polymer SS-injection, the total rate was varied. This was to keep the polymer velocity (shear rate) approximately constant. Adjusted for the applied shear rate in the core the apparent viscosity was set equal to the bulk viscosity, 7 cP.
3. Polymer fractional flow was derived and compared with the water fractional flow curve revealed a shift to higher water saturation.
4. Polymer will reduce the water permeability. The permeability reduction, RRF, was not measured, but from previous work with this type of polymer, RRF is in the range of 2 to 3. With polymer viscosity of 7 cP, the endpoint relative water permeability was 0.153, yielding  $RRF = 3.3$ . Fractional flow curves with polymer viscosity of 7 cP and RRF of 1.0 (no permeability reduction) and  $RRF = 1.5$  and  $RRF = 2.0$  were derived. As can be seen,  $RRF = 1.5$  seems to match the experimental fractional flow, while in the final part of the experiments,  $RRF = 2$  seems to be a better match. This is in agreement with the plugging tendency, as seen in *Figure 7-8*.

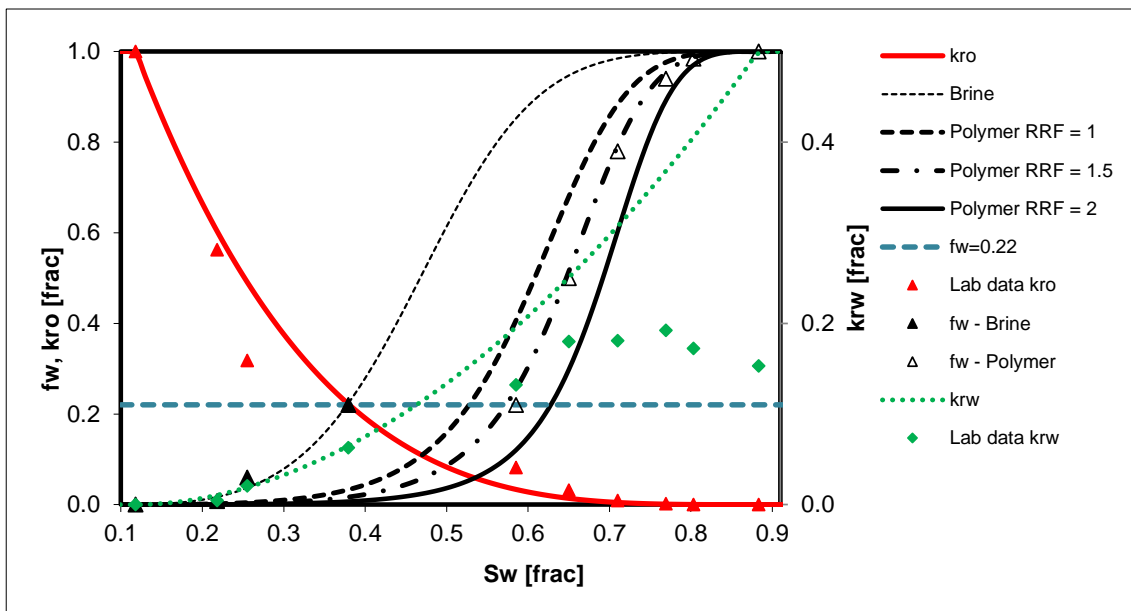


Figure 7-8: Measured and estimated fractional flow

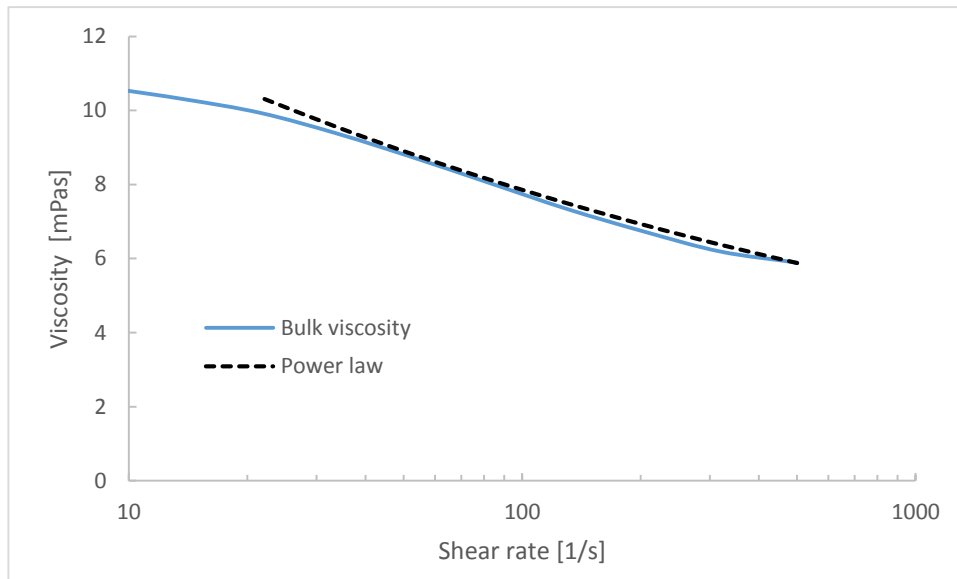


Figure 7-9: Polymer bulk viscosity fitted with a power law dependency

Figure 7-9 shows the bulk viscosity vs. shear rate. The applied shear rate in the core can be estimated from the polymer velocity, see Table 7-3. The polymer shear rate was in the range of 140 to 230  $\text{s}^{-1}$ , which from Figure 7-9 corresponds to viscosity in the range of 7.4 to 6.7 cP.

In conclusion, this type of SS-experiment clearly demonstrates the effect of improving the sweep efficiency by increasing the viscosity of the injected water. It also reveals the EOR mechanisms of polymer flooding; improved sweep efficiency by reducing the mobility, increasing the viscosity and reducing the water permeability.

This work also addresses the potential of performing EOR screening as part of a standard SCAL program.

Finally, the experimental data will be utilized in IOR simulation.

## 8 APPENDIX

### Appendix A List of symbols

$f_g$	...	Gas flow fraction; $f_g = q_g/q_t$ , where $q_g$ is the gas flow rate and $q_t$ is the total flow rate.
$f_o$	...	Oil flow fraction; $f_o = q_o/q_t$ , where $q_o$ is the oil flow rate and $q_t$ is the total flow rate.
$f_w$	...	Water flow fraction; $f_w = q_w/q_t$ , where $q_w$ is the water flow rate and $q_t$ is the total flow rate.
$k$	mD	Permeability.
$k_{el}$	mD	Klinkenberg corrected gas permeability (equivalent liquid).
$k_g$	mD	Permeability to gas at 100 % gas saturation.
$k_o$	mD	Permeability to oil at 100 % oil saturation.
$k_o(S_{wi})$	mD	Permeability to oil at initial water saturation. It is common to measure $k_o(S_{wi})$ at different conditions, or with different oil, for instance; at ambient, at ambient temperature at ncp, or, at reservoir conditions.
$k_o(S_{wr})$	mD	Permeability to oil at residual water saturation.
$k_{REF}$	mD	Reference permeability. In most cases, this is the permeability to oil at initial saturation measured immediately before flooding or centrifugation.
$k_{Tol}$	mD	Permeability to Toluene at 100% Toluene saturation.
$k_r$	frac.	Relative permeability, $k_r \equiv k/k_{REF}$ .
$k_{ro}(S_w)$	frac.	Relative permeability to oil as a function of water saturation.
$k_{rw}(S_w)$	frac.	Relative permeability to water as a function of water saturation.
$k_w$	mD	Permeability to water at 100% water saturation.
$k_w(S_{orw})$	mD	Permeability to water at residual oil saturation on completion of an imbibition [IDC] process.
$L_c$	cm	Core (or plug) length.
$p$	bar	Pressure.
$q_g$	mL/min	Gas flow rate.
$q_o$	mL/min	Oil flow rate.
$q_t$	mL/min	Total flow rate; $q_t = q_w + q_o + q_g$ .
$q_w$	mL/min	Water flow rate.

$S$	frac.	Saturation; the volume of one fluid or phase as a fraction of the total pore space.
$S_g$	frac.	Gas saturation; the volume of gas as a fraction of the total pore space.
$S_{gr}$	frac.	Residual gas saturation resulting after spontaneous imbibition of water.
$S_L$	frac.	Liquid saturation; the volume of liquid as a fraction of the total pore space.
$S_o$	frac.	Oil saturation; the volume of oil as a fraction of the total pore space.
$S_{or}$	frac.	Residual oil saturation at the end of a process where oil saturation (monotonously) decrease.
$S_{org}$	frac.	Residual oil saturation at the end of a gas drainage [CDI] process.
$S_{orw}$	frac.	Residual oil saturation at the end of a water imbibition [IDC] process.
$S_w$	frac.	Water saturation; the volume of water as a fraction of the total pore space.
$\langle S_w \rangle$	frac.	Average water saturation.
$S_{wi}$	frac.	Initial water saturation. Denotes the saturation achieved after a primary drainage (starting from 100 % water saturation).
$S_{wr}$	frac.	Residual water saturation. Water saturation achieved after a secondary drainage (e.g.; after the Amott D process).
$T$	°C	Temperature.
$V$	mL	Volume.
$V_B$	mL	Core (or plug) bulk volume (includes pore space and grain volume).
$V_p$	mL	Core or plug (connected) pore volume.
$V_{pHe}$	mL	Core or plug (connected) pore volume determined by Helium porosimetry.
$V_{pinj}$	“PV”	Pore volumes injected.
$\Delta\rho_{og}$	g/mL	Density contrast between oil and gas, $\Delta\rho_{og} = \rho_o - \rho_g$ .
$\delta_w$	...	Displacement-by-water ratio, $\delta_w \equiv V_{AA}/(V_{AA} + V_{AB})$ .
$\delta_o$	...	Displacement-by-oil ratio, $\delta_o \equiv V_{AC}/(V_{AC} + V_{AD})$ .
$\mu_o$	cP	Viscosity of oil.
$\mu_w$	cP	Viscosity of water.
$\rho_o$	g/mL	Density of oil.
$\rho_w$	g/mL	Density of water.
$\phi$	frac.	Porosity; volume of (connected) pore space as a fraction of the bulk core (or plug) volume.
$\phi_{Mohr}$	frac.	Porosity as derived from pore volume obtained by Nitrate water flooding and Mohr's titration.

$\phi_{He}$	frac.	Porosity as derived from Helium porosimetry.
$\sigma$	mN/m	Interfacial tension.
$\sigma_{ow}$	mN/m	Interfacial tension between SFW and oil.



## **Appendix B Acronyms and special terms**

ISSM	In-situ saturation measurement (here: X-ray transmission measurement, 1-Dimensional).
NCP	Net confining pressure, the difference between the pressure exerted by the confinement fluid of the core holder on the rubber sleeve and the pressure in the pores of the core.
n.m.	not measured
SCAL	Special Core Analysis.
SFW	Synthetic Formation water, composed to coincide as close as possible to the water present in the formation.
SS	Steady-state, a method for determining relative permeability by flooding two or three immiscible fluids simultaneously into the core. Different saturations are set up at different combinations of the simultaneous flow rates.

## **Appendix C Steady-state Relative Permeability Measurement**

### **C.1 Introduction: Steady-state relative permeability**

In two-phase steady-state relative permeability measurement, two fluid phases are pumped simultaneously through the core. A gas/water imbibition starts from an initial water saturation,  $S_{wi}$ ; by flooding gas at several rates to establish the reference permeability,  $k_g(S_{wi})$ . Next, the water pump and the gas pump operates simultaneously, at a very low water flow fraction (such as  $f_w = 0.008$ ), continuing until a steady-state, as defined by stable differential pressure and no more change of saturation, is achieved. The first steady-state relative permeability value is then determined from the saturation derived from the volume balance and the measured differential pressure. The process is continued with monotonously increasing water flow fractions, resulting in increasing water saturation. Finally, only water is flowing,  $f_w = 1$ , and the saturation on completion of this flooding is designated the residual gas saturation,  $S_{grw}$ .

Inverting the steady-state data through the Darcy relation presumes that saturation profiles are homogeneous. However, there are always capillary discontinuities in a core flooding, such as at the core-to-end-piece contact, and consequently there will be saturation profiles. Using high flow-rates will reduce the effect of the discontinuity by making viscous forces dominating the capillary forces. Extending the core length also reduce the relative influence of the capillary end-effects.

Measuring in-situ saturation (ISSM), that is; the saturation profile along the core, allow for detection of saturation distribution effects relating to capillary discontinuities. ISSM, thus, provides a quality control for the steady state experiments.

It is possible to remove much of the remaining bias caused by capillary effects (and inhomogeneity) by applying core flood history matching tools (such as Sendra). Typically, such tools use different parametric “models” for the relative permeability (such as Corey or LET) and for the capillary pressure (such as Skjæveland or LET) and a core flood simulator. In essence, the tool will vary the parameters in these “model” until the simulator output match the measured experimental “history” (such as capillary pressure versus time and produced fluid versus time). It is also possible to include saturation profiles as part of the “historical” data.

### **C.2 Apparatus Overview**

The Apparatus for two-phase Steady state flooding, as outlined in *Figure 8-1* operates at reservoir conditions, pumps the two fluids simultaneously through the core, and recirculates the fluids. Average saturations in the core are deduced from volume balance calculations; (i) the total amount of fluids in the system is known and fixed, (ii) the amount of fluids in the pumps and in the separator are precisely known or measured at any time, and then (iii) the difference between the two is the amount of fluids within the pore space. Saturation profiles are deduced from measurements with an X-ray transmission measurement system.

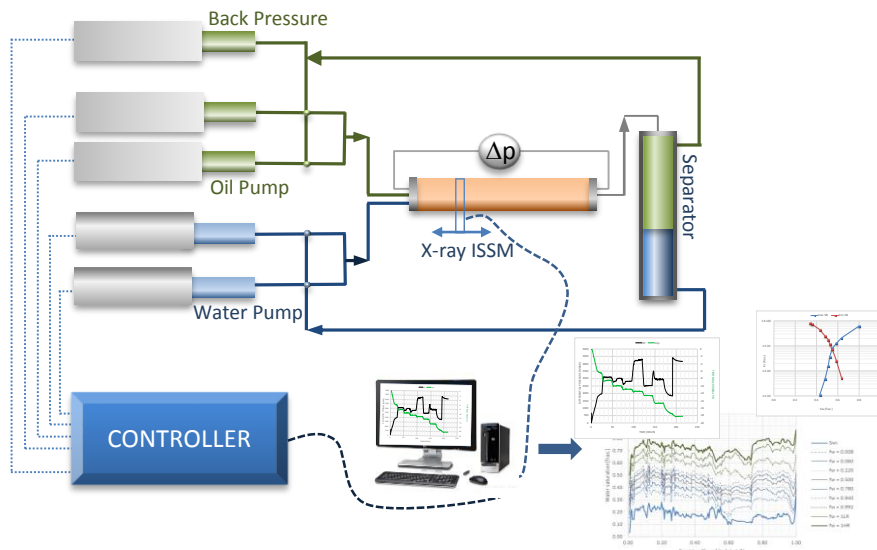


Figure 8-1: Apparatus for Two-phase Steady State Core Flooding.

### C.3 Pumping System

**The pumping system** consists of five computer controlled cylinders that have the capability of recycling two phases simultaneously through a core sample. The cylinders are paired, and two cylinder pairs are used for recycling water and oil (or a gaseous phase). Each fluid is pumped into the core sample with accurate and virtually pulse free flow rates. For each of the cylinder pairs, one cylinder delivers fluid into the sample, while the other receives fluid through the return line from the separator. The fifth cylinder is working in a constant pressure mode, and acts as a back pressure regulator within 50 mbar accuracy. This cylinder is connected to the oil (or gas) return line, but is in contact with both phases indirectly through the separator. It provides an excellent back pressure control. The flow rates are adjustable from 0.001 ml/min to 10 ml/min.

### C.4 Fluid Separator

Effluent from the core is flooded into a sapphire tube where the fluids settle into separate phases. The separator is always kept at the same temperature and pressure as the core, pumps, and tubing. As shown in *Figure 8-2*, the sapphire tube is protected by a steel “cage”, while several access tubes allows entry of effluent from the core as well as withdrawal of the each of the separated fluids. The case illustrated in *Figure 8-2* is relevant for the water/oil flooding.

The amount of gas, oil, and water in the sapphire tube is monitored by photographing the separator at fixed intervals. A computer program is used after completion of the flooding test to read through all the images and detect the position of the menisci, and thus the volume of the phases present in the separator. Accuracy is in the range of  $\pm 0.1 \text{ cm}^3$ .

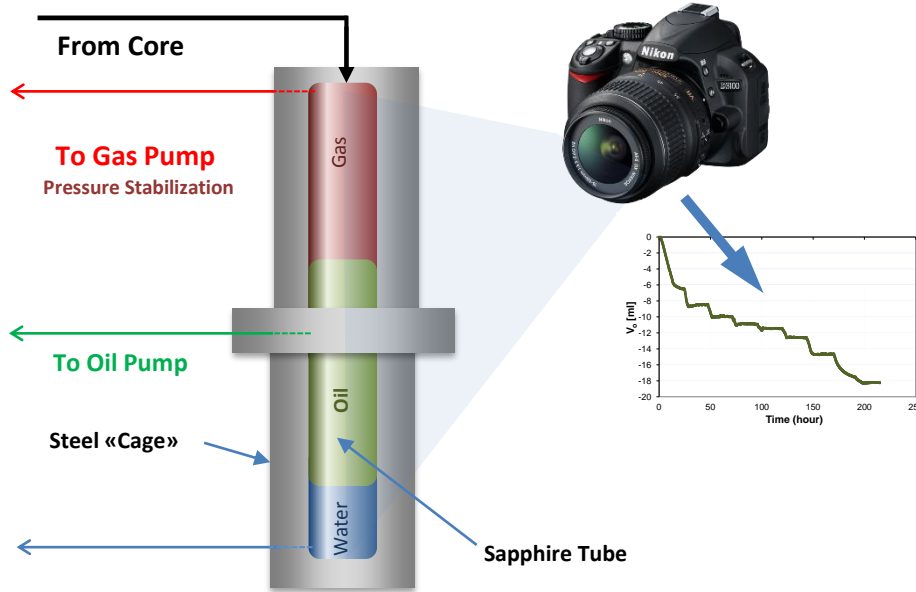


Figure 8-2: Separator used in recirculating core flood system.

### C.5 Hydrostatic core holder

A **hydrostatic core holder** is used in the apparatus, see Figure 8-3. The outlet distribution end piece is of conventional type with three concentric rings and cross-hatch every 45°. A wire screen is placed on the outlet distribution end piece to minimize particle washout and to ensure uniform fluid flow across the outlet end face. The core sample is completely covered with Teflon tape, alumina foil and a Viton sleeve.

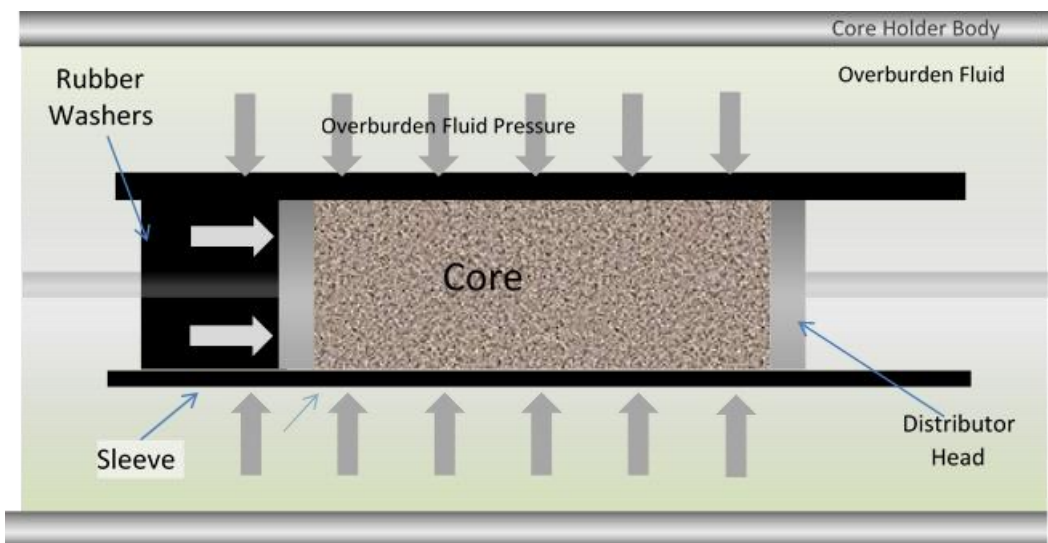


Figure 8-3: Hydrostatic Core Holder – Principle.

## C.6 Pressure difference

The **pressure drop** across the core sample is measured by two high resolution differential pressure transmitters with adjustable range. The maximum range is zero to 5 bar for one transmitter and zero to 300 mbar for the other transmitter, and the accuracy is within 0.1 % of the calibrated range.

The pumps, the separator and the core holder are all placed in a heating cabinet, and provide a closed loop for recycling of both phases under high pressure and high temperature up to 690 bar and 160 °C. The apparatus is capable of running either steady-state type experiments or unsteady-state type experiments, i.e. either one or two phases can be simultaneously injected into the core sample. The monitoring of the apparatus and data acquisition (pressures, volumes, flow rates etc.) are automated and performed by a computer.

## C.7 Water/Oil Kr SS – Flooding apparatus.

In the water/oil steady state flooding, the core starts out at initial water saturation,  $S_{wi}$ , as established by draining the whole core through a water-wet porous plate. Only water and oil are present in the pore space. *Figure 8-4* shows the flooding rig set-up for a water/oil Kr SS process.

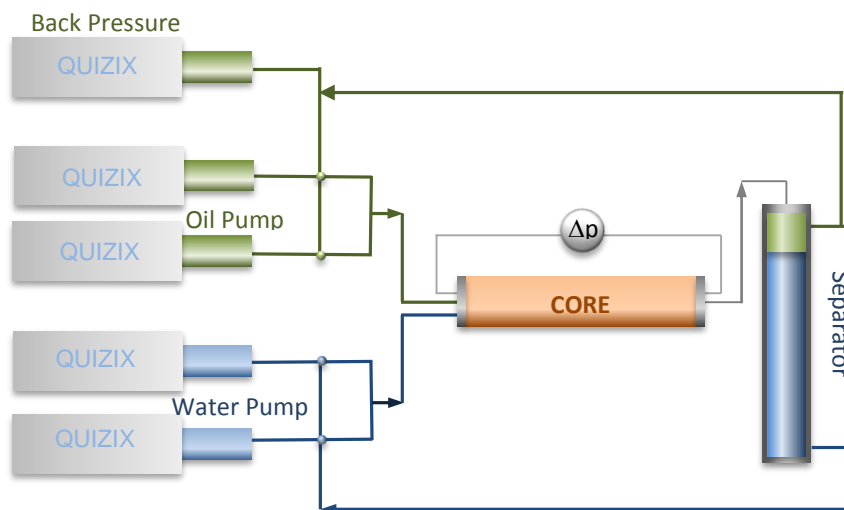


Figure 8-4: Water/Oil Kr SS flooding rig

Two pump cylinders are filled with synthetic formation water, these cylinders act as the water pump. Three pump cylinders are filled with oil, one cylinder is used to control the “back-pressure”, which is essentially the pressure at the outlet end of the core. The remaining two pump cylinders are used as the oil pump. The separator is filled with oil and water, and as the

first process is expected to cause a reduction of the oil saturation in the core, the initial water level in the separator is high.

The test itself consist in:

- Oil flooding.** To establish the reference permeability for calculations of relative permeabilities, oil is flooded at several rates.  $k_{REF} = k_o(S_{wi})$ .
- IDC<sub>2</sub> flooding.** Oil and SFW are flooded simultaneously at several monotonously increasing water flow fractions.
- Each flow fraction is allowed to continue until the differential pressure stabilizes and no further production of oil is observed.
- The set of water flow fractions is selected to attain a reasonable distribution of saturations, typically  $f_w = \{0.008, 0.060, 0.220, 0.500, 0.780, 0.920, 0.994\}$ .
- Going from one water flow-fraction to the next is done by ramping, that is; the water flow rate is increased linearly with time while the oil rate is decreased linearly with time until the desired flow rates are achieved. The ramping time may be several hours, and is the same for water flow rate and oil flow rate.
- The total flow rate is adjusted to a level that is expected to yield an optimal (with respect to the measurement range of the differential pressure transmitters) range of pressure differentials over the core.
- q<sub>w</sub> Upstep .** On completion the final simultaneous oil and water flow, a set of two single phase water floodings are made. These two are designated as  $f_w = 1LO$  ("low" rate single phase water flood) and  $f_w = 1HI$  ("high" rate single phase water flood). The average saturation in the core after completion of the  $f_w = 1HI$  is designated the residual oil saturation after water-flood,  $S_{orw}$ .
- The permeability to water determined at the end of the  $f_w = 1HI$  is the  $k_w(S_{orw})$ .